JASON

12

B.S.

Technical Report JSR-76-14 *June 1977*

LIMITS ON COHERENT PROCESSING DUE TO INTERNAL WAVES

By: R. F. DASHEN S. M. FLATTÉ W. H. MUNK F. ZACHARIASEN

Contract No. DAHC15-73-C-0370
ARPA Order No. 2504
Program Code No. 3K10
Date of Contract: 2 April 1973
Contract Expiration Date: 30 November 1977
Amount of Contract: $3,176,255

Sponsored by

DEFENSE ADVANCED RESEARCH PROJECTS AGENCY
1400 WILSON BOULEVARD
ARLINGTON, VIRGINIA 22209
ARPA ORDER NO. 2504

STANFORD RESEARCH INSTITUTE
Menlo Park, California 94025 · U.S.A.

Copy No. .....

UNCLASSIFIED

SECURITY CLASSIFICATION OF THIS PAGE (When Data Entered)

REPORT DOCUMENTATION PAGE

READ INSTRUCTIONS BEFORE COMPLETING FORM

1. REPORT NUMBER: JSR 76-14

2. GOVT ACCESSION NO.:

3. RECIPIENT'S CATALOG NUMBER:

4. TITLE (and Subtitle): LIMITS ON COHERENT PROCESSING DUE TO INTERNAL WAVES.

5. TYPE OF REPORT & PERIOD COVERED: Technical Report

6. PERFORMING ORG. REPORT NUMBER: SRI - JSR-76-14

7. AUTHOR(s): R. F. Dashen, S. M. Flatté, W. H. Munk and F. Zachariasen

8. CONTRACT OR GRANT NUMBER(s): DAHC15-73-C-0370, ARPA Order-2504

9. PERFORMING ORGANIZATION NAME AND ADDRESS:
Stanford Research Institute
333 Ravenswood Avenue
Menlo Park, California 94025

10. PROGRAM ELEMENT, PROJECT, TASK AREA & WORK UNIT NUMBERS: SRI Project 3000

11. CONTROLLING OFFICE NAME AND ADDRESS:
Defense Advanced Research Projects Agency
1400 Wilson Boulevard
Arlington, Virginia 22209

12. REPORT DATE: May 1977

13. NO. OF PAGES: 36

14. MONITORING AGENCY NAME & ADDRESS (if diff. from Controlling Office): 28p.

15. SECURITY CLASS. (of this report): UNCLASSIFIED

15a. DECLASSIFICATION/DOWNGRADING SCHEDULE:

16. DISTRIBUTION STATEMENT (of this report)

Approved for public release; distribution unlimited

Jun 77

17. DISTRIBUTION STATEMENT (of the abstract entered in Block 20, if different from report)

18. SUPPLEMENTARY NOTES

19. KEY WORDS (Continue on reverse side if necessary and identify by block number)

OCEAN WAVES	SIGNAL PROCESSING
SPECTRA	ACOUSTIC EMISSION SIGNAL PROCESSING
RECEIVERS	ACOUSTIC PROCESSING
ACOUSTIC SOUND SOURCES	ACOUSTIC SIGNAL PROCESSING TECHNIQUES

20. ABSTRACT (Continue on reverse side if necessary and identify by block number)

We derive estimates of the effects produced by internal waves in the ocean on coherent spatial and temporal processing of acoustic signals based on the empirical Garret-Munk GM75 internal wave spectrum. We present results for horizontal and surface limited rays, for point and array receivers, and for stationary and moving sources.

are derived on

are presented

DD FORM 1 JAN 73 1473

EDITION OF 1 NOV 65 IS OBSOLETE

UNCLASSIFIED

SECURITY CLASSIFICATION OF THIS PAGE (When Data Entered)

332 500

LB

ABSTRACT

We derive estimates of the effects produced by internal waves in the ocean on coherent spatial and temporal processing of acoustic signals based on the empirical Garrett-Munk GM75 internal wave spectrum. We present results for horizontal and surface limited rays, for point and array receivers, and for stationary and moving sources.

CONTENTS

I. INTRODUCTION

This report addresses itself to the question of what limits sound speed fluctuations in the ocean place on the dimensions and integration times of acoustic arrays. We shall for the present defer any discussion of advanced processing techniques, and confine ourselves to the simple case of an array that measures incident intensity from various angles by adding linearly varying phase shifts to the hydrophones in the array, and by integrating the received signal over some period of time. We investigate at what array dimensions and at what integration time coherent processing is destroyed by sound speed fluctuations induced by the ocean medium. The results obtained for this situation will serve as a convenient baseline against which to measure the improvements that may be obtainable through the use of more sophisticated processing techniques.

II. COHERENT PROCESSING AND THE PHASE STRUCTURE FUNCTION

Let us assume that we have a receiver consisting of a vertical rectangular array of hydrophones of horizontal and vertical lengths y and z with a density of n hydrophones per unit area. Let us further assume that there is a source located at a horizontal bearing angle θ_0 (relative to the array normal) emitting an acoustic frequency σ_0. Then in the absence of perturbations induced by the ocean, the receiver would pick up a signal

$$\sum_{\alpha=1}^{N} \psi^{(\alpha)} \int_0^Y dy \int_0^Z dz \int_0^T dt\, e^{iqy(\sin\theta_0-\sin\theta)}\, e^{-i(\sigma_0-\sigma)t} \tag{2.1}$$

if it integrates for a time T at a frequency σ and is looking in the horizontal direction θ. Here α indexes the different acoustic rays along which the signal can travel from source to receiver and $\psi^{(\alpha)}$ is the complex signal associated with ray α. The acoustic wave number q is defined by $q = c/\sigma_0$ where c is the sound speed at the receiver.

In general, the ocean medium through which the signal travels will disturb the received signal so that the signal associated with each ray path α will vary from one hydrophone to another, and will vary with time. Thus $\psi^{(\alpha)}$ becomes replaced by $\psi^{(\alpha)}(\vec{x},t)$, and hence, when averaged over an ensemble of oceans, the received intensity from direction θ at frequency σ will be

$$\langle I(\theta,\sigma)\rangle = n^2 \sum_{\alpha\,\alpha'} \int_0^Y dy \int_0^Y dy' \int_0^Z dz \int_0^Z dz' \int_0^T dt \int_0^T dt'$$

$$e^{iq(\sin\theta_0-\sin\theta)(y-y')}\, e^{-i(\sigma_0-\sigma)(t-t')}\, \langle \psi^{(\alpha)}(\vec{x},t)^* \psi^{(\alpha')}(\vec{x}',t')\rangle \tag{2.2}$$

The fluctuations induced by the ocean along two different rays are independent. Hence $\langle \psi^{(\alpha)*}\psi^{(\alpha')}\rangle = \langle\psi^{(\alpha)}\rangle^* \langle\psi^{(\alpha')}\rangle$ for $\alpha \neq \alpha'$. These averages are proportional to $e^{-1/2\ \Phi^{(\alpha)^2}}\ e^{-1/2\ \Phi^{(\alpha')^2}}$ (see Ref. 1). When the fluctuations are large $\Phi^{(\alpha)^2}$ and $\Phi^{(\alpha')^2}$ are large and terms with $\alpha \neq \alpha'$ contribute little to the received intensity.

For terms with $\alpha = \alpha'$ we have[1)]

$$\langle \psi^{(\alpha)}(\vec{x},t)^*\ \psi^{(\alpha)}(\vec{x}',t')\rangle = I^{(\alpha)}\ e^{-\frac{1}{2}\ D(\vec{x}-\vec{x}',\ t-t')},$$

where D is the phase structure function and $I^{(\alpha)}$ is the intensity average of ray α. To a good approximation D is independent of ray and we shall assume this henceforth. Thus

$$\langle I(\theta,\sigma)\rangle = n^2 \sum_{\alpha} I^{(\alpha)} \int_0^Y dy \int_0^Y dy' \int_0^Z dz \int_0^Z dz' \int_0^T dt \int_0^T dt'$$

$$e^{iq(\sin\theta_0-\sin\theta)(y-y')}\, e^{-i(\sigma_0-\sigma)(t-t')}\, e^{-\frac{1}{2}\ D(\vec{x}-\vec{x}',\ t-t')}, \tag{2.3}$$

and our problem is reduced to the study of the behavior of D.

Before proceeding to do this, however, let us anticipate what we will learn about D to give an estimate of when coherent processing fails.

First, we note that as either the spatial or temporal separations go to infinity, $D \to 2\Phi^2$ where Φ^2 is the parameter defined in Ref. 1, and which coincides with the mean square phase fluctuation along a ray when the fluctuation is small. Thus Φ^2 sets the basic scale of D.

If Φ^2 is sufficiently small, then D is everywhere small and there is no limit on coherent processing. To make a numerical estimate of when this occurs, we note[1] that for an axis ray

$$\Phi^2 = \left(\frac{\nu}{50\ \text{Hz}}\right)^2 \left(\frac{R}{300\ \text{km}}\right) \quad ,$$

where R is the propagation range and ν is the acoustic frequency. The region in R and ν where $\Phi^2 < 1$, where coherent processing is always valid, is shown in Fig. 1.

When R and ν are such that $\Phi^2 > 1$, limits on coherent processing become meaningful. In this case only small spatial or temporal receiver separations are relevant and (as will be shown later) D is essentially quadratic in the separations. Hence, taking for simplicity the case of a point receiver integrating over time, we may set

$$D(0,t-t') = \Phi^2 \left(\frac{t-t'}{\tau}\right)^2 \tag{2.4}$$

where τ is some characteristic time. With this form for D, we may now evaluate the integral in (2.3) (for $\theta = \theta_0$, $\sigma = \sigma_0$) and we find

$$\langle I(T) \rangle = \int_0^T dt \int_0^T dt'\, e^{-\frac{1}{2} D(0,t-t')}$$

$$= \begin{cases} \dfrac{\tau T \sqrt{2\pi}}{\Phi} & T \text{ large} \\ T^2 & T \text{ small} \end{cases} \tag{2.5}$$

A schematic plot of the integral as a function of T is shown in Fig. 2. The dotted line represents the true behavior, interpolating smoothly between the two asymptotic expressions given in eq.(2.5). A reasonable definition of where

coherent processing fails is where the two asymptotic forms meet; this occurs at $T = \tau\sqrt{2\pi}/\phi$. At this value of T, $D(0,T) = 2\pi$. Thus we shall use $D = 2\pi$ as our criterion for the failure of coherent processing.

III. GENERAL FORMULAE FOR THE PHASE STRUCTURE FUNCTION

The calculation of the phase structure function D can be carried out as follows. The most general situation is one in which we are comparing two rays joining two distinct sources to two distinct receivers, (Fig. 3). We shall label the rays 1 and 2; ray 1 joins a source at $\vec{x}_{S1}$ to a receiver at $\vec{x}_{R1}$ and ray 2 connects a source at $\vec{x}_{S2}$ to a receiver at $\vec{x}_{R2}$. Let x_1 and x_2 be horizontal distance along rays 1 and 2 respectively; then $(x_1, y_1(x_1), z_1(x_1))$ and $(x_2, y_2(x_2), z_2(x_2))$ denote points on the two rays. We therefore have $(x_{S1}, y_1(x_{S1}), z_1(x_{S1})) = (x_{S1}, y_{S1}, z_{S1})$ and $(x_{R1}, y_1(x_{R1}), z_1(x_{R1})) = (x_{R1}, y_{R1}, z_{R1})$, with analogous expressions for ray 2.

The phase structure function for these two rays is defined by

$$D(1,2) = \left\langle \left(q \int_{\text{ray } 1} \frac{\delta c}{c}\, ds - q \int_{\text{ray } 2} \frac{\delta c}{c}\, ds \right)^2 \right\rangle \quad . \tag{3.1}$$

In Ref. 1 it is shown that when the two rays are not far apart, and when the sound-speed fluctuations are dominated by internal waves, (3.1) may be replaced by

$$D(1,2) = 2 \int_0^R dx \int_0^\infty dk \int_0^\infty d\omega \, \frac{F(k,\omega;\, z(x))}{k_y} \left[1 - \cos\Delta t \cos(k_y \Delta y(x) + k_z \Delta z(x))\right] \quad . \tag{3.2}$$

where $\Delta y(x)$ and $\Delta z(x)$ are the horizontal and vertical separations of the two rays at a horizontal distance x along the rays, and $\Delta t = t_1 - t_2$ is the time separation of the rays, and $F(k,\omega;\, z(x))$ is the internal-wave spectrum. The spatial separations of source and receiver come in through the boundary conditions on $\Delta y(x)$ and $\Delta z(x)$:

$$\Delta y(0) = y_{S1} - y_{S2} \equiv Y_S, \quad \Delta y(R) = y_{R1} - y_{R2} \equiv Y_R$$

$$\Delta z(0) = z_{S1} - z_{S2} + \tan\theta(0)(x_{S1}-x_{S2}) \equiv Z_S + \tan\theta(0)X_S \ ,$$

$$\Delta z(R) = z_{R1} - z_{R2} + \tan\theta(R)(x_{R1}-x_{R2}) \equiv Z_R + \tan\theta(R)X_R \ .$$

Since the deterministic sound speed c(z) varies only vertically, we have an explicit expression for $\Delta y(x)$, namely:

$$\Delta y(x) = Y_S + (Y_R - Y_S)\ x/R \quad . \tag{3.3}$$

The quantity $\Delta z(x)$ is defined as the solution of the differential equation

$$\frac{d^2}{dx^2}\Delta z(x) + \frac{1}{c^2}\left[\frac{d^2}{dz^2}\ c(z(x))\right]\Delta z(x) = 0 \quad , \tag{3.4}$$

subject to the boundary conditions given above.

As an illustration, suppose the sound channel is parabolic: $c(z) = c + 1/2\ K^2(z-\bar{z})^2$, where $\bar{z}$ is the sound channel depth. Then the differential equation for $\Delta z(x)$ has the solution

$$\Delta z(x) = \frac{(Z_R+\tan\theta(R)X_R)\sin Kx + (Z_S+\tan\theta(0)X_S)\sin K(R-x)}{\sin KR} \quad . \tag{3.5}$$

More generally, the solution to the differential equation for $\Delta z(x)$ can be written

$$\Delta z(x) = \alpha\tan\theta(x) + \beta\tan\theta(x) \int_0^x \frac{dx'}{(\tan\theta(x))^2} \quad ,$$

where the constants α and β are to be determined from the boundary conditions given earlier. For very long ranges, when there are many loops in the ray, the integral over dx' becomes nearly proportional to x. Thus, we have, approximately,

$$\Delta z(x) = \tan\theta(x)\left[\left(\frac{Z_S + \tan\theta(0)X_S}{\tan\theta(0)}\right)\left(\frac{R-x}{R}\right) + \left(\frac{Z_R + \tan\theta(R)X_R}{\tan\theta(R)}\right)\left(\frac{x}{R}\right)\right] . \tag{3.6}$$

The quantities k_y and k_z in (3.2) are given by the internal-wave dispersion relations:

$$k_y = k\sqrt{\frac{\omega^2 - \omega_L^2}{\omega^2 - \omega_i^2}} \tag{3.7}$$

$$k_z = k\,\frac{n(z)}{\sqrt{\omega^2 - \omega_i^2}} \quad , \tag{3.8}$$

where $\omega_L^2 = \omega_i^2 + n^2\theta^2$. Here $n(z)$ is the buoyancy frequency and ω_i is the inertial frequency. The Garrett-Munk 75 model of the internal-wave spectrum is

$$\frac{F(k,\omega;\, z(x))}{k_y} = 8\,\langle\mu_0^2\rangle\,\frac{1}{\left(\sum_{j=1}^{\infty}\frac{1}{j^2+j_*^2}\right)}$$

$$\frac{q^2\omega_i\, n^3}{B\, n_0^4}\;\frac{\omega^2-\omega_i^2}{\omega^3}\;\frac{1}{k}\sqrt{\frac{\omega^2-\omega_i^2}{\omega^2-\omega_L^2}}$$

$$\frac{1}{k^2 + \left(\frac{\pi j_*}{B}\right)^2\frac{\omega^2-\omega_i^2}{n_0}}$$

$$\theta(n-\omega)\,\theta(\omega-\omega_L)\,\theta\left(k - \frac{\pi}{B}\frac{\sqrt{\omega^2-\omega_i^2}}{n_0}\right) \quad . \tag{3.9}$$

This spectrum is normalized by the requirement that the parameter Φ is

$$\Phi^2 = \int_0^R dx \int_0^\infty dk \int_0^\infty d\omega\, \frac{F(k,\omega;z(x))}{k_y} \quad . \tag{3.10}$$

Here $\langle \mu_0^2 \rangle$ is the mean square sound speed fluctuation at the surface (actually at the bottom of the mixed layer), j_* is a mode number cutoff, q is the (sound axis value of the) acoustic wave number, n_1 is the buoyancy frequency on the sound axis, n_0 is the buoyance frequency at the surface, ω_i is the inertial frequency and B is the vertical scale depth. Canonical numerical values of these are:

$$(\mu_0)_{rms} = 4.9 \times 10^{-4} \qquad n_1/2\pi = 1.1 \text{ cph}$$

$$j_* = 3 \qquad n_0/2\pi = 3 \text{ cph}$$

$$\omega_i/2\pi = 1/24 \text{ cph}$$

$$B = 1 \text{ km} \quad .$$

The θ functions in (3.9) limit the ranges of integration in (3.10), and in particular exclude singularities at $\omega = 0$ and $k = 0$.

Expressions similar to (3.10) obtain if we use, for example, ω and mode number j as independent variables:

$$D(1,2) = 2 \int_0^R dx \sum_{j=1}^{\infty} \int_0^{\infty} d\omega \, \frac{F(\omega,j;z(k))}{k_y}$$

$$[1 - \cos\omega\Delta t \ \cos(k_y \Delta y(x) + k_z \Delta z(x))] \quad , \qquad (3.11)$$

where now we replace k_y and k_z by

$$k_y = \frac{j\pi}{B} \frac{\sqrt{\omega^2 - \omega_L^2}}{n_0} \quad , \quad k_z = \frac{j\pi}{B} \frac{n}{n_0} \quad .$$

Again the normalization is such that

$$\Phi^2 = \int_0^R dx \sum_{j=1}^{\infty} \int_0^{\infty} d\omega \, \frac{F(\omega,j;z(x))}{k_y} \quad , \qquad (3.12)$$

and, for the GM75 spectrum, we have

$$\frac{F(\omega,j;z(x))}{k_y} = \frac{8}{\pi^2}\langle\mu_0^2\rangle \frac{1}{\sum_{j=1}^{\infty}\frac{1}{j^2+j_*^2}} \cdot \frac{i}{j}\frac{1}{j^2+j_*^2}$$

$$\frac{q^2 B\ \omega_i\ n^3}{n_0^2\ \omega^3}\sqrt{\frac{\omega^2-\omega_i^2}{\omega^2-\omega_L^2}}\ \theta(n-\omega)\theta(\omega-\omega_L) \quad . \tag{3.13}$$

IV. INDIVIDUAL SMALL SEPARATIONS AND THEIR CONTRIBUTIONS TO D

We are primarily interested in cases where the parameter Φ^2 is large, corresponding to the saturated or partially saturated regimes, for only here will there be limitations on coherence. For this case we only need evaluate the phase structure function for small spatial and temporal separations, since the contribution of large separations in eq.(2.3) is heavily damped by the large value of Φ^2. When the separations are small, their effect in D is additive, so we may discuss each of them separately. We shall find that the general formulae for D, given in the previous section, become relatively simple when the separations are small, and we will end up with a rather simple analytic expression for D characterized primarily by coherence lengths for temporal and vertical and horizontal spatial separations. Let us outline how this comes about.

A. Temporal Separations

The general expression for D reduces to

$$D(T) = 2\int_0^R dx \int_0^\infty dk \int_0^\infty d\omega\ \frac{F(k,\omega;z(x))}{k_y}(1-\cos\omega T) \quad . \tag{4.1}$$

For small T we replace $1 - \cos\omega T$ by $1/2\ \omega^2 T^2$ so that

$$D(T) = \dot{\Phi}^2 T^2 \quad , \tag{4.2}$$

where $\dot{\phi}^2$ is defined in Ref. 1. Finally, we write this as

$$D(T) = 2\phi^2 \cdot \left\{\frac{1}{2}\left(\frac{T}{\tau}\right)^2\right\} \quad , \tag{4.3}$$

with the coherence time τ defined simply by

$$\tau = \frac{\phi}{\dot{\phi}} \quad . \tag{4.4}$$

For an axis ray, this time is[1)]

$$\tau^2 = 2\omega_i^2 \log n_1/\omega_i = 0.45 \text{ (hours)}^{-2} \quad \tau = 1.6 \text{ hours} \; .$$

B. Vertical Spatial Separations

Here it is most convenient to use the ω-j language:

$$D(Z) = 2 \int_0^R dx \sum_{j=1}^{\infty} \int_0^{\infty} d\omega \, \frac{F(\omega,j;z(x))}{k_y} \, (1 - \cos k_z \Delta z(x)) \quad . \tag{4.5}$$

(Z, the length of a vertical receiver, comes into this formula through the boundary conditions on $\Delta z(x)$). Here

$$k_z = \frac{j\pi}{B} \frac{n(z(x))}{n_0} \quad . \tag{4.6}$$

The value of using ω and j as variables is that k_z depends only on j, and in fact is simply linear in j. Because of this fact, and because $F(\omega,j;z(x))$ is proportional to $1/j(j^2 + j_*^2)$, the sum on j can be approximately evaluated analytically, we replace $\sum_j$ by $\int dj$, and define

$$I(\alpha,j_*) \equiv \int_{j_0}^{\infty} dj \, \frac{1}{j} \frac{1}{j^2+j_*^2} \cos \alpha j \Big/ \int_{j_0}^{\infty} dj \, \frac{1}{j} \frac{1}{j^2+j_*^2} = \frac{1}{\log \frac{j^2+j_*^2}{j_0^2}} \Big\{ - 2 \, \mathrm{Ci}\,(\alpha j_0)$$

$$+ [\cosh \alpha j_* (\mathrm{Ci}\,(\alpha(j_0+ij_*)) + \mathrm{Ci}\,(\alpha(j_0-ij_*)))]$$

$$+ i[\sinh \alpha j_* (\mathrm{Si}\,(\alpha(j_0+ij_*)) - \mathrm{Si}\,(\alpha(j_0-ij_*)))] \Big\} \quad , \tag{4.7}$$

where Ci and Si are the cosine and sine integral functions. We can set $j_0 = 1$ here, to correspond to $\sum_{j=1}^{\infty}$.

In terms of the function I, the phase structure function can now be written

$$D(Z) = 2 \int_0^R dx \left[\sum_j \int d\omega \frac{F(\omega,j;z(x))}{k_y}\right] \left(1 - I\left(\frac{\pi}{B} \frac{n(x)}{n_0} \Delta z(x),\ j_*\right)\right) \quad . \tag{4.8}$$

A simplified formula, valid for small separations, is obtained by expanding the function I for small Δz:

$$D(Z) = 2 \int_0^R dx \left[\sum_j \int d\omega \frac{F(\omega,j;z(x))}{k_y}\right] \frac{1}{2} \left(\frac{\Delta z}{\ell_v}\right)^2 \left[\log \frac{\Delta z}{\ell_v} + \gamma_v\right] , \tag{4.9}$$

where ℓ_v is an x-dependent length defined by

$$\ell_v(x) = \frac{B}{2\pi} \frac{\sqrt{\log(j_*^2+1)}}{j_*} \frac{n_0}{n(z(x))} \quad , \tag{4.10}$$

and where γ_v is a constant given by

$$\gamma_v = \frac{3}{2} - C - \log \frac{x}{\sqrt{\log(j_*^2+1)}} \quad , \tag{4.11}$$

where C - 0.577... is Euler's constant.

The expression (4.9) for D can be evaluated analytically for a near axis ray. For these rays the sound channel is nearly parabolic, and the rays are therefore nearly sinusoidal. Thus (cf eq.(3.5) with $\theta_R = \theta_S = Z_S = 0$ and $Z_R = Z$)

$$\Delta z(x) = Z \frac{\sin Kx}{\sin KR} \quad . \tag{4.12}$$

Using this formula in (4.9), and noting that $F(k,\omega;z(x))$ is not a function of x for the axis ray, we find

$$D(Z) = 2\Phi^2 \left\{\frac{1}{2} \left(\frac{Z}{\mathcal{L}_v}\right)^2 \left(\log \frac{Z}{\mathcal{L}_v} + \Gamma_v\right)\right\} \quad , \tag{4.13}$$

where the coherence length $\mathcal{L}_v$ for this ray is

$$\mathcal{L}_v = \sqrt{2}\ \bar{\ell}_v$$

($\bar{\ell}_v$ here is ℓ_v evaluated on the sound axis) and the constant Γ_v is

$$\Gamma_v = \frac{1}{2} + \gamma_v - \frac{1}{2} \log 2 \quad .$$

Numerically, we find

$$\ell_v = 300 \text{ meters},$$

and

$$\Gamma_v = 1.49.$$

Eq.(4.9) for D can also be evaluated analytically for a steep ray, because for such rays the major contribution to the integral comes from the region near the ray apex.

For a single apex, we can replace the quantity

$$\frac{1}{2}\left(\frac{\Delta z}{\ell_v}\right)^2 \left(\log \frac{\Delta z}{\ell_v} + \gamma_v\right) \quad ,$$

in the integrand by its value at the apex. The remaining integral then gives just the parameter $2\Phi^2$ evaluated in the apex approximation. Thus

$$D(1,2) = \Phi^2 \left(\frac{\Delta \hat{z}}{\hat{\ell}_v}\right)^2 \left(\log \frac{\Delta \hat{z}}{\hat{\ell}_v} + \gamma_v\right) \quad . \tag{4.14}$$

where the hat on Δz and ℓ_v indicate that they are to be evaluated at the ray apex $(\hat{x},\hat{z})$. (Note that γ_v is independent of (x,z), so we do not have to indicate any special point at which it is to be evaluated.)

For very long ranges, where a steep ray has many apexes, we can use (3.7) to calculate Δz. For example, for a point source and a vertical receiver of height Z,

$$\Delta z(x) = \frac{\theta(x)}{\theta(R)} \cdot \frac{xZ}{R} \quad ,$$

where we have replaced $\tan\theta$ by θ since all angles are small, and where Z_R is Z. With this approximation we cannot simply evaluate Δz at the apex, because vanishes there. Rather we must average $\Delta z^2 \propto \theta^2$ over the ray apex. This yields the expression

$$D(Z) = \Phi^2 \cdot \frac{1}{3} \frac{\bar{\theta}^2}{\theta(R)^2} \left(\frac{Z}{\hat{\ell}_v}\right)^2 \left(\log \frac{Z}{\hat{\ell}_v} + \gamma_v\right) \quad , \tag{4.15}$$

where the average of θ^2 over an apex is

$$\bar{\theta}^2 = \sqrt{\frac{32}{\pi^3}} \frac{\omega_i}{n_0} \sqrt{\frac{n_0^2 B}{n^2(\hat{z}) r}} \quad , \tag{4.16}$$

where r is the radius of curvature of the ray at the apex. An obvious modification of (4.15) gives the expression for D for arbitrary source and receiver separations as in eq.(3.7).

We may put eq.(4.14) into a form parallel to eq.(4.12) by choosing

$$\mathcal{L}_v = \sqrt{3}\, \hat{\ell}_v \sqrt{\frac{\overline{\theta^2(R)}}{\bar{\theta}^2}} \quad , \tag{4.17}$$

as the coherence length for a steep ray, and

$$\Gamma_v = \gamma_v + \log \frac{\mathcal{L}_v}{\hat{\ell}_v} \quad . \tag{4.18}$$

Numerically, for the surface limited ray, $\mathcal{L}_v$ = 420m and Γ_v = 3.

C. Horizontal Spatial Separations

Now we have

$$D(Y) = 2 \int_0^R dx \sum_{j=1} \int_0^\infty d\omega \frac{F(\omega, j; z(x))}{k_y} (1 - \cos k_y \Delta y(x)) \quad , \tag{4.19}$$

where

$$\Delta y(x) = Y\, x/R$$

for a horizontal receiver of length Y. Furthermore,

$$k_y = \frac{j\pi}{B} \frac{\sqrt{\omega^2 - \omega_L^2}}{n_0} \quad .$$

Unfortunately, in contrast to case B, k_y is now not a function of j alone. An analytic evaluation of (4.19) can therefore not be carried very far. It is still possible to carry out the sum on j, obtaining an analog of (4.8); however, the ω integration is now prohibitively difficult. As a result, simple expressions analogous to (4.9) and (4.13) are not now obtainable.

Nevertheless, as we shall see in the following section, a fairly good (30%) analytic representation of D(Y) is

$$D(Y) = 2\Phi^2 \frac{1}{2} \left\{ \left(\frac{Y}{\mathcal{L}_H} \right)^2 \right\}$$

where the horizontal coherence length $\mathcal{L}_H$ is 6.4 km.

SUMMARY

Combining these separations we have the following simple approximate expression for D, valid for small separations.

$$D = 2\Phi^2 \left\{ \frac{1}{2} \left(\frac{T}{\tau} \right)^2 + \frac{1}{2} \left(\frac{Y}{\mathcal{L}_H} \right)^2 + \frac{1}{2} \left(\frac{Z}{\mathcal{L}_V} \right)^2 \left(\log \frac{Z}{\mathcal{L}_V} + \Gamma_V \right) \right\} . \qquad (4.20)$$

with $\tau = 1.6$ hours

and for near axis rays

$$\mathcal{L}_V = 300 \text{ m},$$

$$\mathcal{L}_H = 6.4 \text{ Km.}$$

and $\Gamma_V = 1.49$,

while for the surface limited ray,

$$\mathcal{L}_V = 420 \text{ m}$$

$$\Gamma_V = 3.$$

V. HORIZONTAL ARRAYS AND STATIONARY POINT SOURCES

As an application of the results obtained so far, let us consider the case of a stationary point source and a horizontal linear receiver. Thus the source separations are all zero and X_R, Z_R are zero as well. Then $\Delta z(x) = 0$ and $\Delta y(x) = Yx/R$ where we write Y for Y_R. From eq. (3.2) we have

$$D(Y,T) = 2 \int_0^R dx \int_0^\infty dk \int_0^\infty d\omega \frac{F(k,\omega;z(x))}{k_y}$$

$$[1 - \cos\omega T \cos\left(k\sqrt{\frac{\omega^2-\omega_L^2}{\omega^2-\omega_i^2}}\ \frac{Yx}{R}\right)] \quad , \tag{5.1}$$

where $T \equiv t_1 - t_2$. To illustrate what this implies we shall specialize to the axis ray $z(x) = 0$. For this ray $\omega_L = \omega_i$, the integral on dx can be carried out, and we find

$$D(Y,T) = 2R \int_0^\infty dk \int_0^\infty d\omega \frac{F(k,\omega;\,0)}{k_y} \left[1 - \cos\omega T \frac{\sin kY}{kY}\right] \quad . \tag{5.2}$$

The expression for D(Y,T) can be easily evaluated numerically. Fig. 4 shows the ratio $D(Y,T)/2\Phi^2$ for various values of T as a function of Y. Fig.5 shows the same ratio as a function of T for various values of Y.

Figures 4 and 5 also show lines representing fits to the exact expression of the form

$$\frac{D(Y,T)}{2\Phi^2} = \frac{1}{2}\left(\frac{T}{\tau}\right)^2 + \frac{1}{2}\left(\frac{Y}{\mathscr{Y}_H}\right)^2 \quad . \tag{5.3}$$

The value $\tau = 1.6$ hours (which we've seen in Section IV is the value of $\Phi/\dot{\Phi}$) is imposed on the fit. The value of $\mathscr{Y}_H$ is selected to optimize the fit and turns out to be 6.4 km.

We may obtain an analytic result for maximum values of T and Y consistent with coherent processing by using eq. (5.3);

$$\left(\frac{T}{\tau}\right)^2 + \left(\frac{Y}{\mathcal{L}_H}\right)^2 = \frac{2\pi}{\Phi^2} \quad . \tag{5.4}$$

For zero integration time this yields a maximum array length of

$$MAL = \frac{\sqrt{2\pi}}{\Phi}\,\mathcal{L}_H \quad , \tag{5.5}$$

which for a near-axis ray gives

$$MAL = 210\ \lambda\sqrt{\frac{1000\ km}{R}} \quad . \tag{5.6}$$

Similarly a maximum integration time can be obtained as

$$MIT = \frac{\sqrt{2\pi}}{\Phi}\,\tau = \frac{MAL}{v} \quad , \tag{5.7}$$

where

$$v = \frac{\mathcal{L}_H}{\tau} = 4\ km/hr \quad . \tag{5.8}$$

For intermediate combinations of array length and integration time limits may be obtained from Figures 4 and 5.

For example, an acoustic frequency of 100 Hz (i.e., an acoustic wavelength of 15 m) at a range of 1000 km yields $\Phi^2 = 26.2$. The line $D/2\Phi^2 = 2\pi/(56.4) = .112$ intersects the T = 0.1 hours curve in Fig. 4 at Y = 3.5 km. Thus for an integration time of 0.1 hours the maximum useful array length is 3.5 km.

VI. MOVING SOURCES

As a final example of the use of the results obtained above, let us discuss the effects of moving sources. For a point source moving with velocity $V = (V_x, V_y, V_z)$, we replace the source dimensions (X_S, Y_S, Z_S) by (V_xT, V_yT, V_zT). We shall confine ourselves to the case of sources moving in the horizontal plane, and set $V_z = 0$. We may then distinguish two possibilities.

A. $V_x = 0$: Source moves transverse to the line joining source to receiver.

In this case we may, as in Section IV, limit ourselves to discussing the axis ray. We then have $\Delta z(x) = 0$, and $\Delta y(x) = V_y T + (Y - V_y T)x/R$ where, as in Section IV, Y is the horizontal dimension of the receiver. Thus. eq. (3.2) becomes replaced by

$$D(Y,T) = 2R \int_0^\infty dk \int_0^\infty d\omega \frac{F(k,\omega;\,0)}{k_y} \left[1 - \cos\omega T \left(\frac{\sin kY - \sin kV_y T}{kY - kV_y T}\right)\right] \tag{6.1}$$

For a point receiver (Y = 0) we therefore find exactly the same results as those given in Section V, but with Y replaced by $V_y T$ so that the maximum integration time in this case is (using our analytic approximation)

$$MIT = \frac{\sqrt{2\pi}}{\Phi} \frac{\tau}{\sqrt{1 + \left(\frac{V_y}{v}\right)^2}} \,. \tag{6.2}$$

Thus the velocity of the moving source adds quadratically to the intrinsic internal-wave velocity, v, to reduce the coherent integration time. The value of V_y at which source motion begins to affect coherent integration is evidently $V_y \sim v = 4$ km/hr. For $Y \neq 0$ evaluation of eq.(6.1) must be done numerically.

B. $V_y = 0$: Source moves directly toward or away from receiver.

We again specialize to a point receiver. Then $\Delta y(x) = 0$ and in calculating $\Delta z(x)$ the boundary conditions are $\Delta z(0) = \tan\theta(0) V_x T$, $\Delta z(R) = 0$. For short integration times T we can add the direct effect of T and the induced Δz due to the source motion. The effect of Δz is given by eq. (4.8).

Insofar as the analytic formula (4.17) is valid one can estimate the maximum integration time T for a point receiver in the same way as in case A, with Z in (4.17) replaced by $V_x T\theta(0)$; T satisfies the equation

$$2\pi = \Phi^2 \left[\left(\frac{T}{\tau}\right)^2 + \frac{V_x T\theta(0)}{\mathcal{L}_v}^2 \left(\log \frac{V_x T\theta(0)}{\mathcal{L}_v} + \Gamma_v\right)\right] \,. \tag{6.3}$$

To estimate the value of V_x at which radial source motion begins to cut into coherent integration time, we may ignore the log term. The relevant velocity is then evidently

$$\frac{1}{\sqrt{\Gamma_v}} \frac{\chi_v}{\theta(0)\tau} \sim .75 \text{ km/hr}$$

for the surface limited ray. This velocity is considerably smaller than the analogous tangential velocity, due to the fact that the shorter vertical coherence length (420 m as compared to 6.4 km) more than compensates for the increase of the critical velocity by the factor $1/\theta(0) \sim 5$. Thus for steep rays radial source motion is a much more serious inhibition to coherent integration than is tangential motion.

In conclusion we should emphasize that the limitations produced by source motion discussed here are only those associated with internal wave induced fluctuations in the ocean. There are also effects produced simply by source motion in the presence of many deterministic multipaths. These have recently been analyzed by H. Cox[2]. (These deterministic multipath effects are of course not relevant for a stationary source.)

References

1. R. F. Dashen et al., JASON report JSS 76-39.

2. H. Cox and E. P. Jensen, "Fluctuations in the Signal Response of the Vertical Array Caused by Source Motion", J. Acc. Soc. Am., 59, 1(A) 1975.

Figure Captions

Fig. 1: The parameter Φ as a function of propagation range and acoustic frequency.

Fig. 2: Schematic plot of received intensity at a point receiver as a function of integration time, showing the transition between the region where coherent processing applies ($I(T) \propto T^2$) and where it fails ($I(T) \propto T$). The time $\tau\sqrt{2\pi}/\Phi$ is the intersection of the small T and large T asymptotic forms for I(T). We say coherent processing is valid below this time.

Fig. 3: Sketch illustrating ray 1, ray 2, the mean ray, and the source and receiver separations projected in the vertical plane. A similar sketch (with straight line rays) applies projected in the horizontal plane.

Fig. 4: Graphs of $D(Y,T)/2\Phi^2$ computed numerically, for various integration times T as a function of horizontal receiver length Y, for a flat ray and a stationary point source. The dotted lines show an approximate fit of the form $D/2\Phi^2 = \frac{1}{2}(T/\tau)^2 + \frac{1}{2}(Y/\mathcal{L}_H)^2$ with $\mathcal{L}_H = 6.4$ km and $\tau = 1.6$ hrs.

Fig. 5: Same as Fig. 4 but plotted as a function of T for various values of Y.

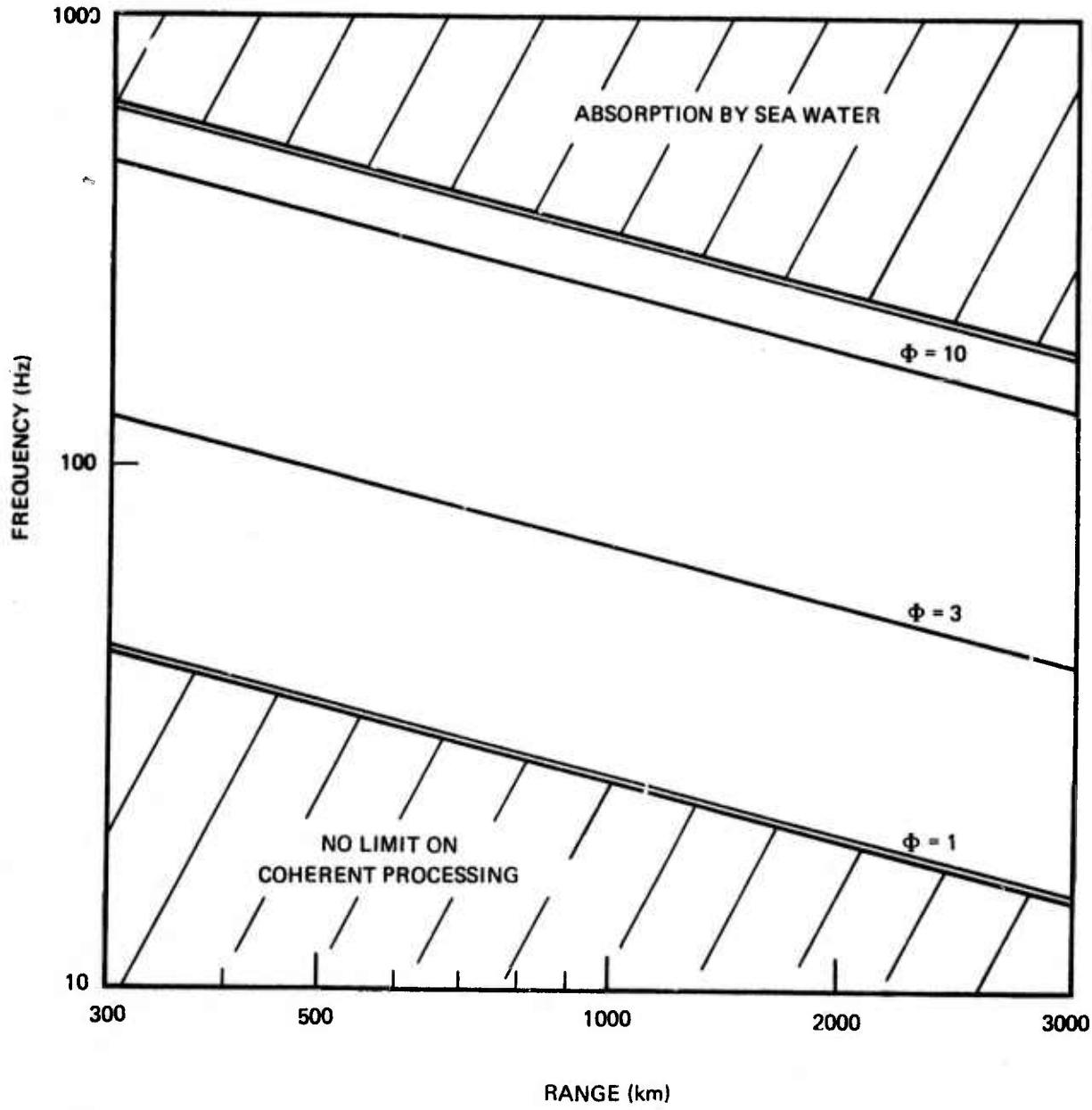
1000
100
10
FREQUENCY (Hz)
ABSORPTION BY SEA WATER
Φ = 10
Φ = 3
Φ = 1
NO LIMIT ON
COHERENT PROCESSING
300
500
1000
2000
3000
RANGE (km)

Figure 1

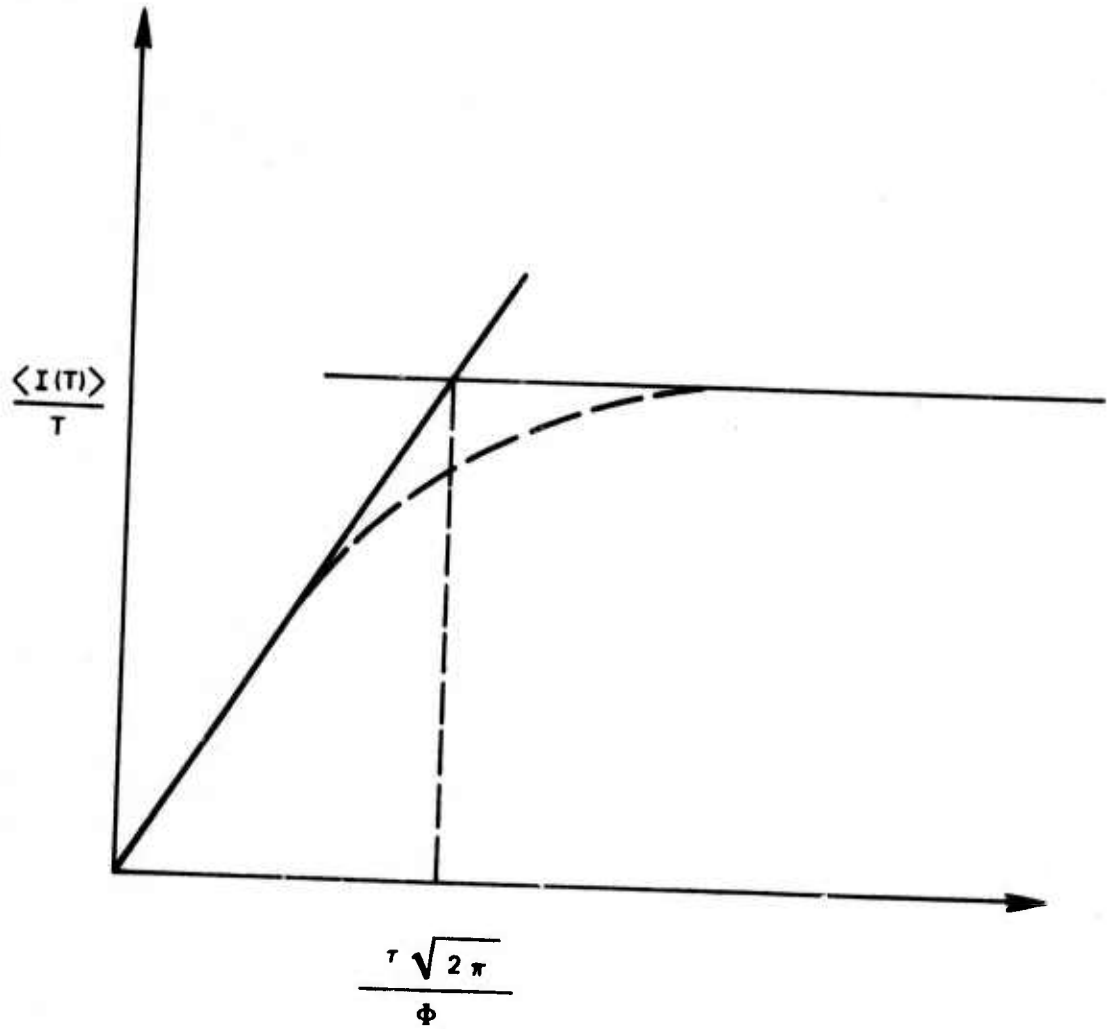
$\frac{\langle I(T) \rangle}{T}$
$\frac{\tau\sqrt{2\pi}}{\Phi}$
INTEGRATION TIME (T)

Figure 2

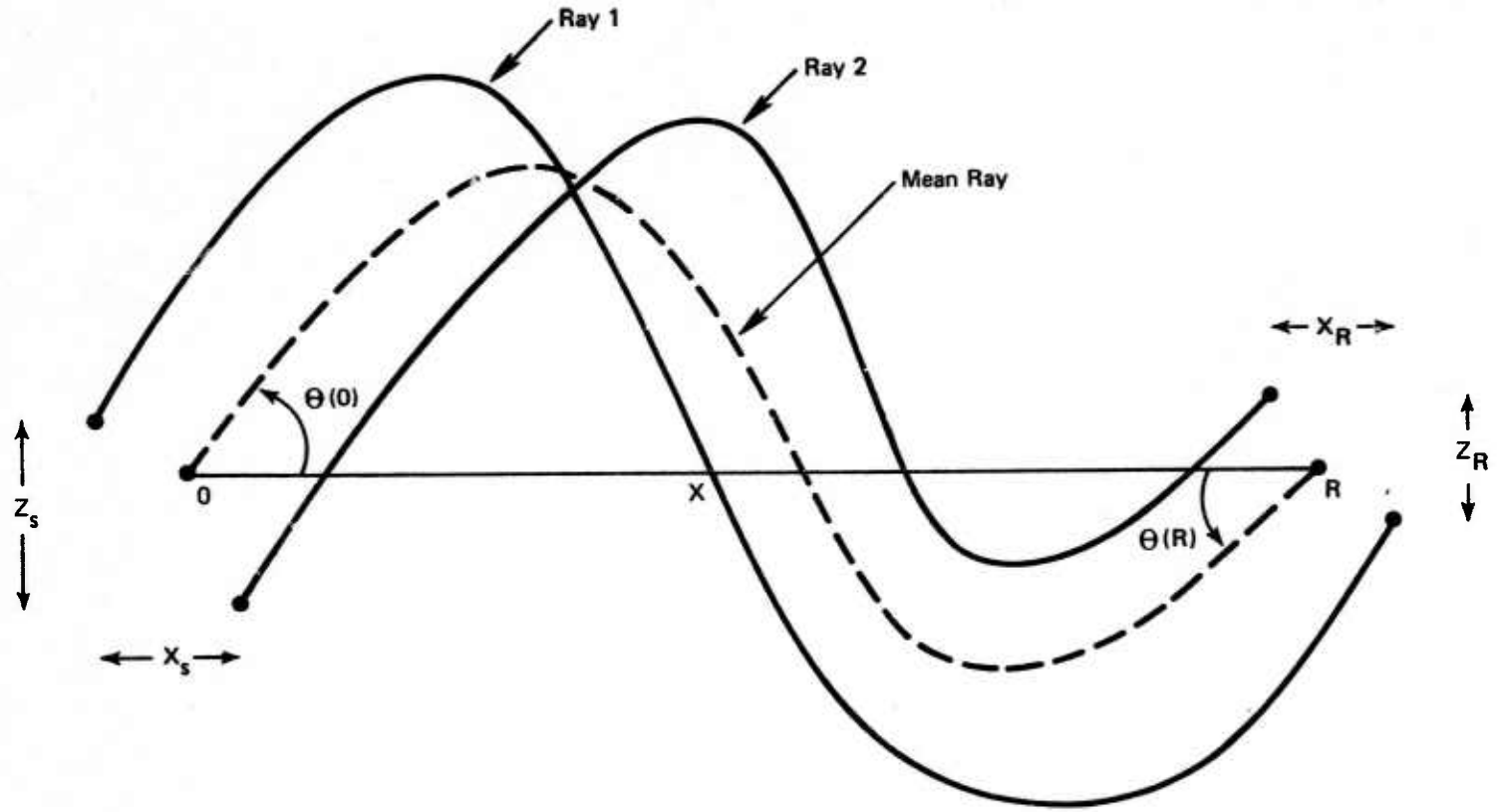

Figure 3

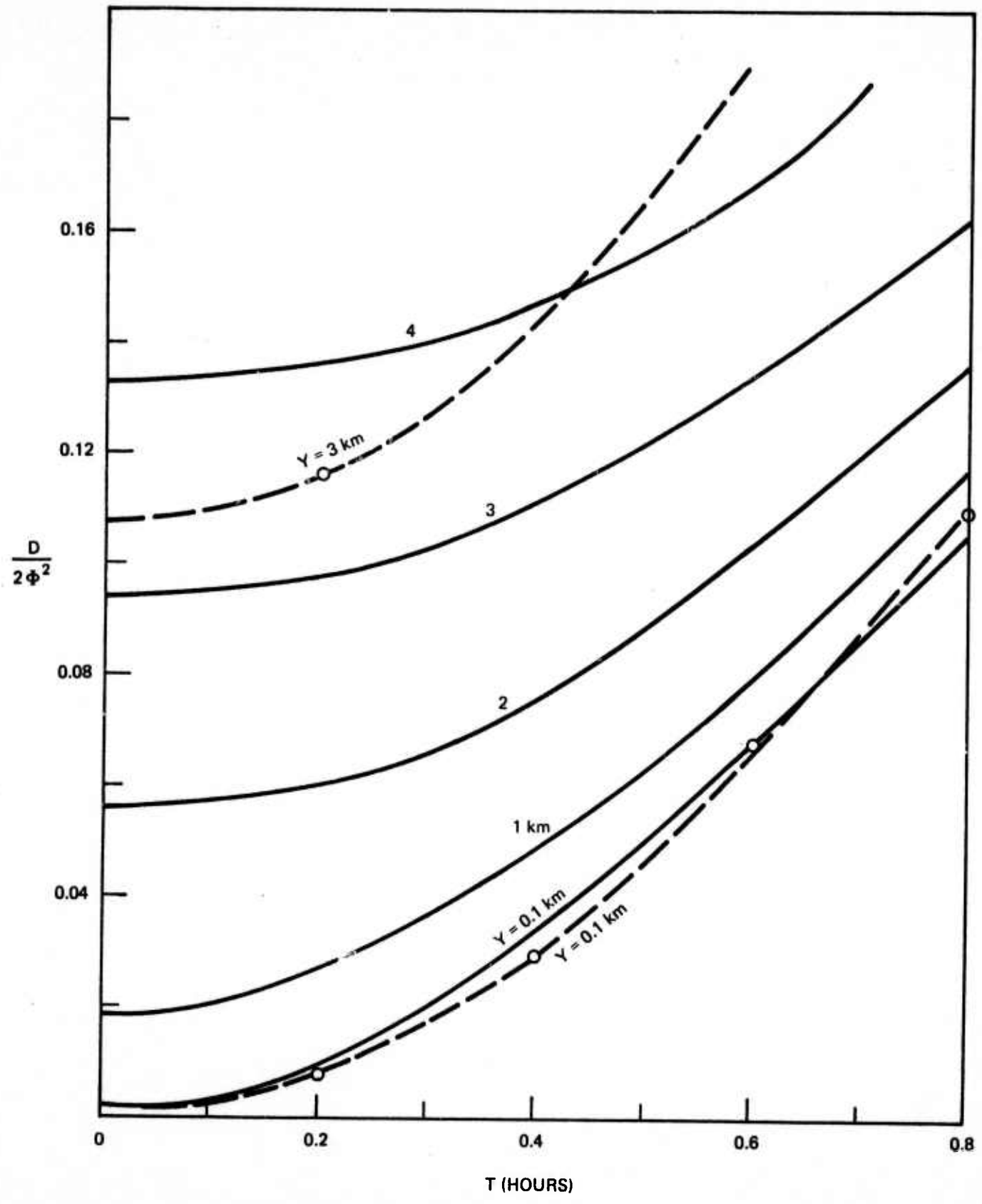
0.16
0.12
0.08
0.04
D / 2Φ²
4
Y = 3 km
3
2
1 km
Y = 0.1 km
Y = 0.1 km
0
0.2
0.4
0.6
0.8
T (HOURS)

Figure 5

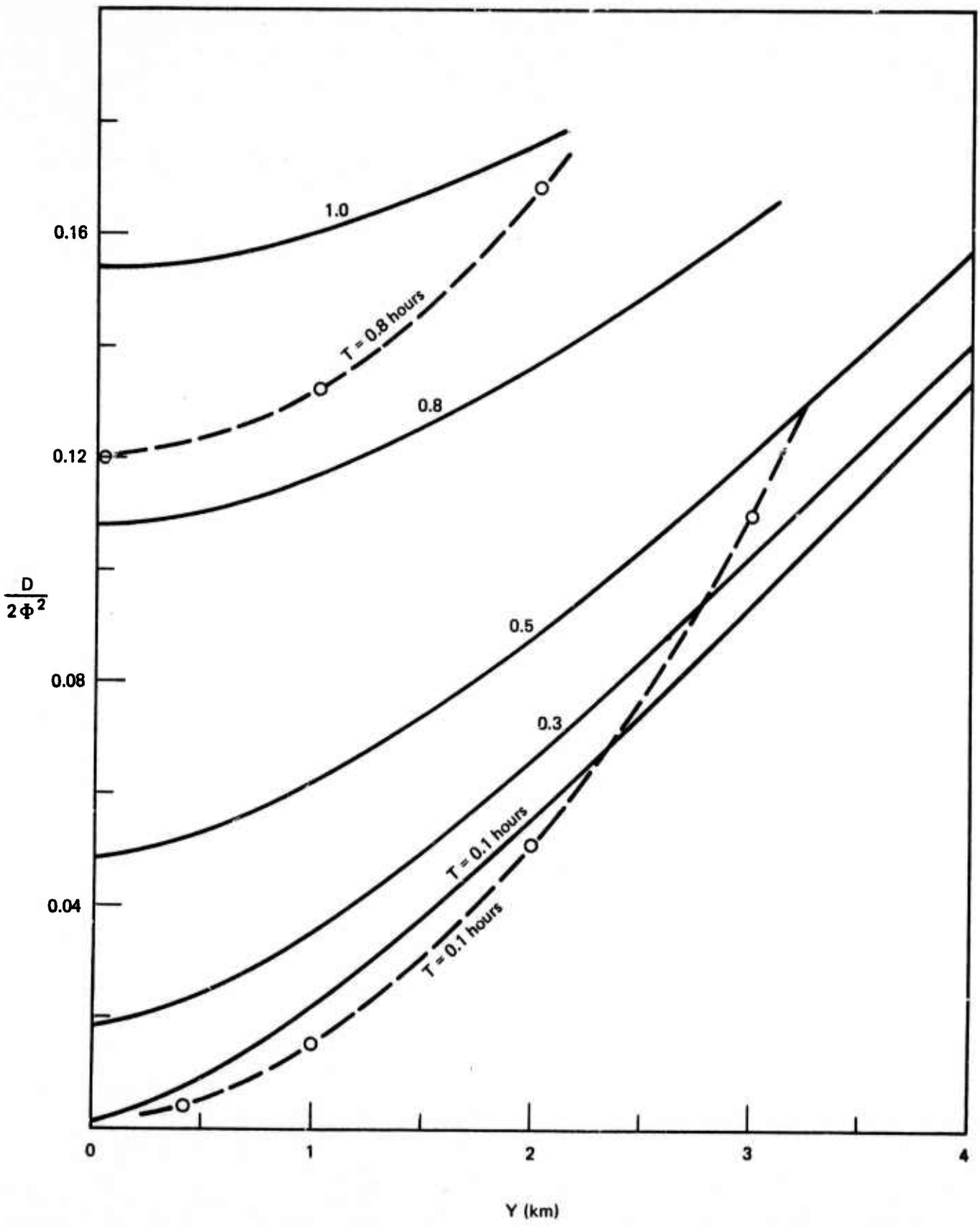
1.0
T = 0.8 hours
0.8
0.5
0.3
T = 0.1 hours
T = 0.1 hours
0.16
0.12
0.08
0.04
D / 2Φ²
0
1
2
3
4
Y (km)

Figure 4

DISTRIBUTION LIST

ORGANIZATION	NO. OF COPIES
Dr. Henry D. I. Abarbanel National Accelerator Laboratory P.O. Box 500 Batavia, Illinois 60510	1
Mr. B. B. Adams Naval Research Laboratory 4555 Overlook Avenue, S.W. Washington, D.C. 20375	1
Dr. V.C. Anderson Scripps Institution of Oceanography University of California La Jolla, California 92037	1
Dr. F. Andrews Catholic University 620 Michigan Avenue, N.E. Washington, D.C. 20017	1
Mr. H.S. Aurand, Jr. Ocean Acoustics Division Naval Ocean Systems Center San Diego, California 92152	1
Mr. James Austin Johns Hopkins University Applied Physics Laboratory Johns Hopkins Road Laurel, Maryland 20810	1
Dr. James E. Barger Bolt, Beranek & Newman, Inc. 50 Moulton Street Cambridge, Massachusetts 02138	1
Mr. C. Bartberger Naval Air Development Center Warminster, Pennsylvania 18974	1
Bell Telephone Laboratories Whippany Road Whippany, New Jersey 07981	2
Dr. Joel Bengston Institute for Defense Analyses 400 Army Navy Drive Arlington, Virginia 22202	1
Dr. A. Berman Naval Research Laboratory 4555 Overlook Avenue, S.W. Washington, D.C. 20375	1
Mr. Ange V. Bernard Manager Anti-Submarine Warfare Systems Project Navy Department Washington, D.C. 20360	1
Dr. H.F. Bezdek Program Director CODE 460 NORDA Bay St. Louis, Mississippi 39529	1
Prof. T.G. Birdsall Cooley Electronics Laboratory Cooley Bldg., North Campus University of Michigan Ann Arbor, Michigan 48105	1
Mr. George L. Boyer Office of Naval Research 800 N. Quincy Street Arlington, Virginia 22217	1
Mr. D.G. Browning New London Laboratory Naval Underwater Systems Center New London, Connecticut 06320	1
Mr. B.M. Buck Polar Research Laboratory, Inc. 123 Santa Barbara St. Santa Barbara, California 93101	1
Dr. H. Bucker Naval Ocean Systems Center San Diego, California 92152	1
Dr. Peter J. Cable Naval Underwater Systems Center New London Laboratory New London, Connecticut 06320	1

ORGANIZATION	NO. OF COPIES
Mr. D. Cacchione Office of Naval Research 495 Summer Street Boston, Massachusetts 02210	1
Dr. Curtis G. Callan, Jr. Department of Physics Princeton University Princeton, New Jersey 08540	1
Lt. Col. G. Canavan DARPA/STO 1400 Wilson Boulevard Arlington, Virginia 22209	1
Mr. G. Cann Room 3D1048 ODDR&E The Pentagon Washington, D.C. 20301	1
Dr. Gerald Carruthers P.O. Box 1925 Main Post Office Washington, D.C. 20013	1
Dr. Kenneth M. Case 2-11037-230 The Rockefeller University New York, New York 10021	1
Dr. Joseph W. Chamberlain 18622 Carriage Court Houston, Texas 77058	1
Mr. Robert M. Chapman Special Assistant Marine Syster Garrett Corporation 9851 Sepulveda Blvd. P.O. 92248 Los Angeles, California 90009	1
Dr. J.G. Clark Institute for Acoustical Research University of Miami 615 SW Second Avenue Miami, Florida 33130	1
Dr. R.H. Clarke Imperial College of Science and Technology Department of Electrical Engineering Exhibition Road London SW7 2BT England	1
Dr. Bernard F. Cole Naval Underwater Systems Center New London Laboratory New London, Connecticut 06320	1
Dr. W.J. Condell Office of Naval Research 800 N. Quincy Street Arlington, Virginia 22217	1
Mr. R. Cooper Office of Naval Research 800 N. Quincy Street Arlington, Virginia 22217	1
Courant Institute 251 Mercer Street New York, New York 10012	2
Dr. C. Cox University of California San Diego 9530 La Jolla Shores Drive La Jolla, California 92937	1
Capt. Henry Cox DARPA/TTO 1400 Wilson Blvd. Arlington, Virginia 22209	1
Mr. J. M. D'Albora Naval Underwater Systems Center Newport, Rhode Island 02840	1
Dr. Roger D. Dashen Institute for Advanced Study Princeton, New Jersey 08540	1

ORGANIZATION	NO. OF COPIES
Dr. S.C. Daubin Rosentiel School of Marine and Atmospheric Science University of Miami Miami, Florida 33149	1
Dr. H. DeFarrari Rosentiel School of Marine and Atmospheric Science University of Miami Miami, Florida 33149	1
Mr. John A. DeSanto Naval Research Laboratory Code 8160 Washington, D.C. 20375	1
Mr. Ferdinand P. Diemer Office of Naval Research 800 N. Quincy Street Arlington, Virginia 22217	1
Mr. F. Dinapoli Naval Underwater Systems Center New London Laboratory New London, Connecticut 06320	1
Mr. J. Dugan Naval Research Laboratory 4555 Overlook Avenue, S.W. Washington, D.C. 20375	1
Prof. I. Dyer MIT Department of Ocean Engineering Cambridge, Massachusetts 02139	1
Prof. Freeman J. Dyson Institute for Advanced Study Princeton, New Jersey 08450	1
Mr. L. Einstein Naval Underwater Systems Center New London Laboratory New London, Connecticut 06320	1
Mr. A. Ellinthorpe Naval Underwater Systems Center New London, Connecticut 06320 ATTN: Code TE	1
Dr. J.O. Elliot Naval Research Laboratory 4555 Overlook Avenue, S.W. Washington, D.C. 20375	1
Mr. J.T. Ewing Lamont-Doherty Geological Observatory Columbia University Palisades, New York 10964	1
Dr. A.G. Fabula Naval Ocean Systems Center San Diego, California 92132	1
Dr. F. Fisher Scripps Institution of Oceanography University of California San Diego La Jolla, California 92037	1
Dr. R.M. Fitzgerald Naval Research Laboratory Department of the Navy Washington, D.C. 20375	1
Dr. Stanley M. Flatte 360 Moore Street Santa Cruz, California 95060	1
Mr. E. Floyd Naval Ocean Systems Center San Diego, California 92132	1
Dr. Henry M. Foley Columbia University Department of Physics New York, New York 10027	1
Mr. H. Freese Naval Underwater Systems Center New London Laboratory New London, Connecticut 06320	1

ORGANIZATION	NO. OF COPIES
Dr. Richard L. Garwin IBM Thos. J. Watson Research Center P.O. Box 218 Yorktown Heights, New York 10598	1
Dr. Roy Gaul Director CODE 600 NORDA Bay St. Louis, Mississippi 39529	1
Mr. A.A. Gerlach Naval Research Laboratory 4555 Overlook Avenue, S.W. Washington, D.C. 20375	1
Dr. C. Gibson University of California San Diego P.O. Box 119 La Jolla, California 92038	1
Dr. Ralph Goodman Technical Director CODE 110 NORDA Bay St. Louis, Mississippi 39529	1
Dr. D. Gordon Naval Ocean Systems Center San Diego, California 92132	1
Dr. O.D. Grace Naval Underwater Systems Center New London Laboratory New London, Connecticut 06320	1
Dr. Richard Gustafson DARPA/TTO 1400 Wilson Boulevard Arlington, Virginia 22209	1
Mr. H. Guthart 404B Stanford Research Institute 333 Ravenswood Avenue Menlo Park, California 94025	1

ORGANIZATION	NO. OF COPIES
Mr. G.R. Hamilton Director, Ocean Research Office CODE 400 NORDA Bay St. Louis, Mississippi 39529	1
Dr. J.S. Hanna Science Applications, Inc. 8400 Westpark Drive McLean, Virginia 22101	1
Mr. R. Hardin Bell Telephone Laboratories Chester, New Jersey 07930	1
Mr. Raymond W. Hasse Naval Underwater Systems Center New London Laboratory New London, Connecticut 06320	1
Cdr. R.K. Hastie NAVMAT-031 Washington, D.C. 20360	1
Dr. E.E. Hays Woods Hole Oceanographic Institution Woods Hole, MA 02543	1
Dr. George H. Heilmeier Director DARPA 1400 Wilson Blvd. Arlington, Virginia 22209	1
Dr. John Brackett Hersey Deputy Assistant Oceanographer for Ocean Science Chief of Naval Research Naval Research Laboratory Washington, D.C. 20390	1
Mr. Robert L. Himbarger ORINCON Corporation P.O. Box 22113 San Diego, California 92122	1

ORGANIZATION	NO. OF COPIES
Dr. Richard Hoglund Operations Research, Inc. 1400 Spring Street Silver Spring, Maryland 20910	1
Dr. C.W. Horton, Sr. Applied Research Laboratory University of Texas P.O. Box Drawer 8029 Austin, Texas 78712	1
Dr. T. Horwath Office of Naval Research 800 N. Quincy Street Arlington, Virginia 22217	1
Mr. B. Hurdle Naval Research Laboratory 4555 Overlook Avenue, S.W. Washington, D.C. 20375	1
Dr. William J. Hurley Center for Naval Analyses 1401 Wilson Blvd. Arlington, Virginia 22209	1
Dr. David Hyde OASN (R&D) Department of the Navy Washington, D.C. 20360	1
Dr. Francis J. Jackson Bolt, Beranek and Newman, Inc. 1701 North Fort Myer Drive Arlington, Virginia 22209	1
Mr. M. Jacobson Rensselaer Polytechnic Institute Department of Mathematics Troy, New York 12181	1
Mr. B. James ARPA/TTO 1400 Wilson Blvd. Arlington, Virginia 22209	1
Mr. Finn Jensen Saclant ASW Research Centre Viale San Bartolomeo 400 I-19026 La Spezia, Italy	1
Mr. William John Jobst Research Scientist Palisades Geophysical Institute 615 SW 2nd Avenue Miami, Florida 33130	1
Dr. Johnathan Katz Department of Astronomy University of California Los Angeles, California 90024	1
Dr. A.I. Kaufman Center for Naval Analyses 1401 Wilson Boulevard Arlington, Virginia 22209	1
Dr. Roger N. Keeler Director of Navy Technology Department of the Navy Washington, D.C. 20360	1
Mr. J. Keller Courant Institute 251 Mercer Street New York, New York 10012	1
Mr. Theo Kooij ARC Director Advanced Research Projects Agency ARPA Research Center Unit 1 Moffett Field, California 94035	1
Dr. N. Kroll University of California San Diego P.O. Box 119 La Jolla, California 92038	1

ORGANIZATION	NO. OF COPIES
Dr. Martin Kronengold Director Institute for Acoustical Research University of Miami 615 SW 2nd Avenue Miami, Florida 33130	1
Cdr. Alan H. Krulish Department of the Navy Office of the Chief of Naval Operations Washington, D.C. 20350	1
Dr. F. Labianca Bell Telephone Laboratories Whippany Road Whippany, New Jersey 07881	1
Mr. R. Lauer Naval Underwater Systems Center New London Laboratory New London, Connecticut 06320	1
Dr. Harold W. Lewis Department of Physics University of California Santa Barbara, California 93106	1
Dr. Bernard Lippmann Dept. of Physics New York University 4 Washington Place New York, New York 10003	1
Dr. Donald J. Looft DARPA 1400 Wilson Boulevard Arlington, Virginia 22209	1
Cdr. Terry J. McCloskey Director CODE 200 NORDA Bay St. Louis, Mississippi 39529	1

ORGANIZATION	NO. OF COPIES
Dr. J. McCoy Naval Research Laboratory 4555 Overlook Avenue, S.W. Washington, D.C. 20375	1
Dr. S. McDaniel Applied Research Laboratory Pennsylvania State University P.O. Box 30 State College, Pennsylvania 16801	1
Mr. Mike McKisic Scientific Officer CODE 460 NORDA Bay St. Louis, Mississippi 39529	1
Dr. G. Maidanik Naval Ship Research and Development Center Washington, D.C. 20007	1
Dr. S.W. Marshall CODE 340 NORDA Bay St. Louis, Mississippi 39529	1
Mr. R.L. Martin Naval Underwater Systems Center New London Laboratory New London, Connecticut 06320	1
Prof. H. Medwin Naval Postgraduate School Department of Physics Monterey, California 93940	1
Mr. R.H. Mellen Naval Underwater Systems Center New London Laboratory New London, Connecticut 06320	1
Dr. M. Milder ARETE Associates 2120 Wilshire Blvd. Santa Monica, California 90903	1

ORGANIZATION	NO. OF COPIES
Dr. J. Miles University of California San Diego P.O. Box 119 La Jolla, California 92038	1
Cdr. A.R. Miller Naval Electronic System Command PME-124 Washington, D.C. 20360	1
Mr. Robert A. Moore DARPA/TTO 1400 Wilson Boulevard Arlington, Virginia 22209	1
Dr. Paul H. Moose Naval Ocean System Center San Diego, California 92152	1
Dr. G.B. Morris University of California Scripps Institution of Oceanography Marine Physical Laboratory San Diego, California 92152	1
Mrs. H. Morris Naval Ocean Systems Center San Diego, California 92132	1
Mr. William A. Moseley Supervisor, Research Physics Naval Research Laboratory 4555 Overlook Avenue, S.W. Washington, D.C. 20375	1
Dr. Richard A. Muller 2831 Garber Berkeley, California 94705	1
Dr. Walter H. Munk 9530 La Jolla Shores Drive La Jolla, California 92037	1
Naval Electronic Systems Command Headquarters Code PME-124 Washington, D.C. 20300	2
Naval Underwater Systems Center ATTN: Technical Library New London Laboratories New London, Connecticut 06320	1
Dr. J. Neubert Naval Ocean Systems Center San Diego, California 92132	1
Dr. William A. Nierenberg Scripps Institution of Oceanography University of California La Jolla, California 92037	1
Mr. J.C. Nolen Institute for Defense Analyses 400 Army Navy Drive Arlington, Virginia 22202	1
Operations Research, Inc. 1400 Spring Street Silver Spring, Maryland 20910	1
Dr. David Palmer Code 8172 Naval Research Laboratory Department of the Navy Washington, D.C. 20375	1
Mr. J. Papadakis Naval Underwater Systems Center New London Laboratory New London, Connecticut 06320	1
Mr. M.A. Pedersen Naval Ocean Systems Center San Diego, California 92132	1

ORGANIZATION	NO. OF COPIES
Dr. Francis W. Perkins, Jr. Plasma Physics Laboratory Princeton University P.O. Box 451 Princeton, New York 08540	1
Dr. O.M. Phillips Hydronautics, Inc. Pindell School Road Howard County Laurel, Maryland 20810	1
Dr. R. Porter Woods Hole Oceanographic Institution Woods Hole, Massachusetts 02543	1
Mr. James H. Probus Director of Navy Laboratories The Pentagon Washington, D.C. 20350	1
Dr. Gordon Raisbeck Arthur D. Little, Inc. Cambridge, Massachusetts 02140	1
Mr. D.J. Ramsdale Acoustics Division Code 8170 Naval Research Laboratory Washington, D.C. 20375	1
Dr. Burton Richter Stanford Linear Accelerator P.O. Box 4349 Stanford, California 94305	1
Mr. W.I. Roderick Naval Underwater Systems Center New London Laboratory New London, Connecticut 06320	1
Mr. Richard R. Rojas Associate Director of Research for Oceanology Naval Research Laboratory Washington, D.C. 20390	1
Dr. Marshall Rosenbluth Institute for Advanced Study Princeton, New Jersey 08549	1
Dr. R. Ruffine ODDR&E The Pentagon Washington, D.C. 20301	1
Capt. Kenneth W. Ruggles Office of the Deputy Director for Research and Engineering (DDR&E) The Pentagon Washington, D.C. 20301	1
Dr. R. Saenger Naval Underwater Systems Center New London Laboratory New London, Connecticut 06320	1
Dr. H. Schenk Naval Ocean Systems Center San Diego, California 92132	1
Dr. M. Schulkin Naval Oceanographic Office Suitland, Maryland 20373	1
Prof. Peter Schultheiss Yale University New Haven, Connecticut 06520	1
Dr. Phil Selwyn ARPA/TTO 1400 Wilson Boulevard Arlington, Virginia 22209	1
Capt. J. Shilling Strategic Systems Project Office Department of the Navy Washington, D.C. 20390	1

ORGANIZATION	NO. OF COPIES
Mr. Carey D. Smith Commander, Naval Sea Systems Command Headquarters Department of the Navy Washington, D.C. 20360 Code 06H1	1
Dr. Gary L. Smith Johns Hopkins University Applied Physics Laboratory Johns Hopkins Road Laurel, Maryland 20810	1
Dr. Preston W. Smith Bolt, Beranek and Newman, Inc. 50 Moulton Street Cambridge, Massachusetts 02138	1
Mr. H. Sonneman Office of the Assistant Secretary of the Navy The Pentagon Washington, D.C. 20360	1
Mr. Glenn R. Spaulding Headquarters, Naval Material Command (MAT034) Washington, D.C. 20360 Room 1044	1
Dr. F. Spiess University of California Scripps Institution of Oceanography Marine Physical Laboratory San Diego, California 92152	1
Dr. R. Spindel Woods Hole Oceanographic Institution Woods Hole, Massachusetts 02543	1
Mr. C.W. Spofford Science Applications, Inc. 8400 Westpark Drive McLean, Virginia 22101	1
Mr. D.C. Stickler Applied Research Laboratory Pennsylvania State University P.O. Box 30 State College, Pennsylvania 16801	1
Dr. M. Strassberg Naval Ship Research and Development Center Washington, D.C. 20007	1
Mr. A.O. Sykes Office of Naval Research Code 412 800 N. Quincy Street Arlington, Virginia 22217	1
Mr. T.E. Talpey Bell Telephone Laboratories Whippany Road Whippany, New Jersey 07981	1
Mr. Frederick Tappert Department of the Navy Office of Naval Research Acoustic & Environmental Support Detachment Arlington, Virginia	1
Capt. Peter R. Tatro, USN Office of the Oceanographer of the Navy 200 Stovall Street Alexandria, Virginia	1
Dr. Alex Thomson Physical Dynamics, Inc. Berkeley, California	1
Mr. Richard D. Trueblood Electronics Engineer Commander Naval Ocean Systems Center San Diego, California 92152	1

ORGANIZATION	NO. OF COPIES
Dr. H. Uberall Catholic University 620 Michigan Avenue, N.E. Washington, D.C. 20017	1
University of Texas Applied Research Laboratory Austin, Texas 78712	2
Mr. R.J. Urick TRACOR, Inc. 1601 Research Blvd. Rockville, Maryland 20850	1
Dr. John F. Vesecky Center for Radar Astronomy Stanford University Stanford, California 94305	1
Dr. William A. Von Winkle Associate Technical Director for Technology Naval Underwater Systems Center New London Laboratory New London, Connecticut 06320	1
Dr. Kenneth Watson Lawrence Berkeley Laboratory University of California Berkeley, California 94720	1
Mr. J. Weileman Courant Institute 251 Mercer Street New York, New York 10012	1
Dr. H. Weinberg Naval Underwater Systems Center New London Laboratory New London, Connecticut 06320	1
Dr. M.S. Weinstein Underwater Systems, Inc. 8121 Georgia Avenue Suite 700 Silver Spring, Maryland 20910	1
Maj. Gen. J.A. Welch, Jr. AFSA 1E 388 The Pentagon Washington, D.C. 20330	1
Capt. J.B. Wheeler Naval Electronic System Command Code 103 Washington, D.C. 20360	1
Mr. H. Wilson Science Applications, Inc. P.O. Box 351 La Jolla, California 92037	1
Dr. J.M. Witting Naval Research Laboratory 4555 Overlook Avenue, S.W. Washington, D.C. 20375	1
Mr. Peter Worcester University of California San Diego E-25 La Jolla, California 92093	1
Dr. J.L. Worzel Marine Science Institute Geophysics Laboratory 700 Thestrand Galveston, Texas 77550	1
Dr. H. Yura Aerospace Corporation P.O. Box 92956 Los Angeles, California 90009	1
Dr. Frederik Zachariasen 452-48 Department of Physics California Institute of Technology Pasadena, California 91109	1